Correlation effects in $4s^04p^6$ and $4s^14p^5$ configurations of krypton studied by the M-NN Auger decay

H. Aksela, S. Aksela, and H. Pulkkinen

Department of Physics, University of Oulu, SF-90570 Oulu 57, Finland

(Received 8 May 1984)

Energy shifts in the M-NN Auger spectrum of krypton caused by strong electron correlation in $4s^04p^6$ and $4s^14p^5$ configurations are studied by comparing the experimental results with the theoretical estimates based on Dirac-Fock multiconfiguration computations.

I. INTRODUCTION

The valence s-hole states of the rare gases, which show strong interaction with certain excited states, have been studied extensively during the last few years.[1–4] Energy shifts from this interaction are found to range from a few to several electron volts for the spectral lines involving outer-shell singly or doubly ionized states, namely ns^1np^6, ns^1np^5, and ns^0np^6. An intense satellite structure is also found to appear on the low-kinetic-energy side of the diagram lines.[1–4]

The experimental outer-shell Auger-electron spectra of the noble gases have been measured by Werme et al.[5] The $L_{2,3}$-MM spectrum of argon and the $M_{4,5}$-NN spectrum of krypton were investigated later in more detail by McGuire[1] and by Dyall and Larkins.[4] Very recently, the

$N_{4,5}$-OO spectrum of xenon was also reinvestigated by Southworth[6] and by our group.[7] Theoretical calculations based on the multiconfiguration Dirac-Fock method were found to reproduce the observed energies of the $N_{4,5}$-OO spectrum of Xe reasonably well.[7] An analogous comparison between experimental and calculated energies of the $M_{4,5}$-NN transitions of Kr will be presented in this paper. These kinds of theoretical approaches have not been used to investigate the $M_{4,5}$-NN transitions of Kr earlier, although a tentative assignment of the lines was presented in Refs. 1 and 4. In order to be able to study the influence of the correlation effects of the energies by carrying out a detailed comparison between theory and experiment, we have remeasured and recalibrated the spectrum by starting from lower energy than Werme et al.[5] and Mehlhorn.[8] Very recently Derenbach and Schmidt[9] reported the elec-
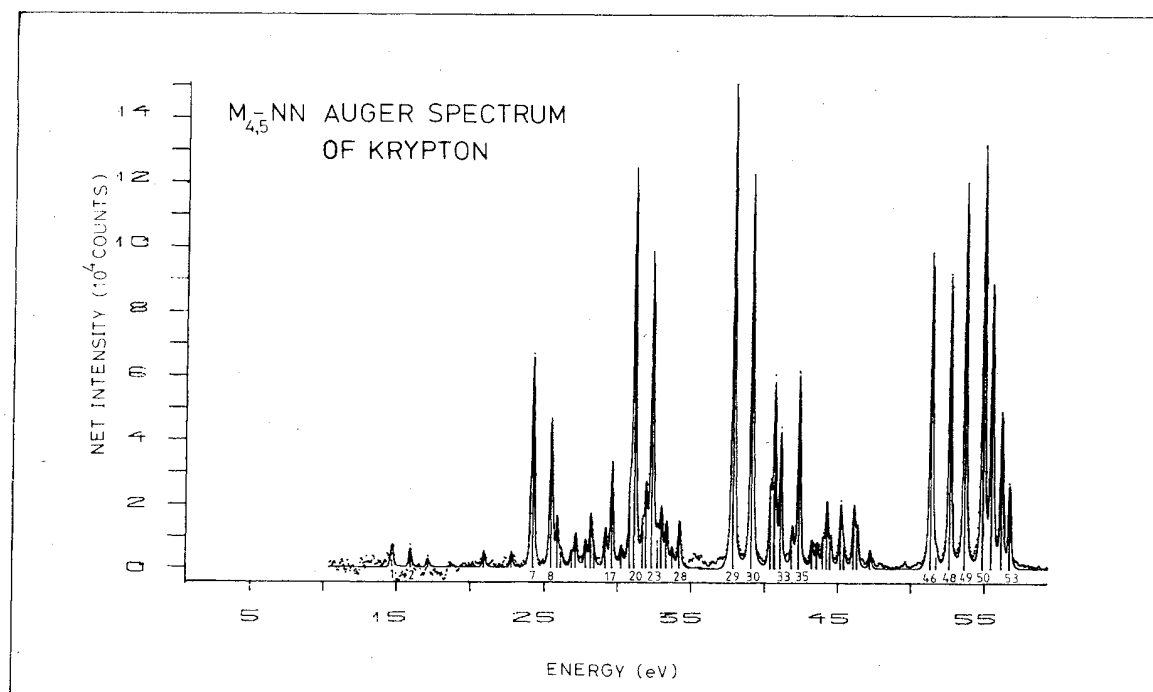
FIG. 1. Experimental Auger-electron spectrum of xenon after background subtraction and dispersion correction. The solid curve and the vertical lines represent a least-squares fit of Voight functions to the experimental points.

2456

tron spectrum of photoionization in Kr, which shows the structure due to the Auger transitions below 20 eV. These authors, however, do not report the energies of the peaks, which are needed for comparison with theory.

II. EXPERIMENT

The $M_{4,5}$-NN Auger spectrum of Kr was measured by means of a cylindrical-mirror spectrometer and with electron-beam excitation.[10]

The energy calibration was carried out with the aid of the M_5-$N_1N_{2,3}(^1P_1)$ and M_4-$N_{2,3}N_{2,3}(^1S_0)$ Auger lines of Kr with energies of 37.837 and 52.577 eV, respectively.[11-14] These lines were chosen as the calibration lines because they are well-separated in the experimental spectrum. The energy values are based on a new value[12] of the ionization potential of Kr II which is given together with the other quantities used in the calibration in Table I. The energy values used earlier[5,8] are thus about 0.2 eV too small, as already pointed out by Hansen[15] and Ohtani et al.[16]

After subtraction of a polynomial background the spectrum was decomposed into the line components by a least-squares fitting procedure. The fit of the experimental spectrum is shown in Fig. 1 and the energies of the main lines obtained from the fit are given in Table II. Energies reported by Werme et al.[5] and by Mehlhorn[8] are also tabulated after applying the correction of 0.2 eV.

After subtraction of the initial-state energy,[13] the energies of the final-state levels are obtained. The energy-level structure of the doubly ionized Kr is depicted in Fig. 2 together with the energy-level structure of Kr III reported in optical spectroscopy.[11]

III. THEORY

The theoretical calculations were carried out with the multiconfiguration Dirac-Fock program of Grant et al.[17] The energies of Auger transitions were obtained as the difference between separately optimized total energies of the singly ionized initial and doubly ionized final-state levels of the Auger process (the ΔSCF approach).

The atomic-state wave function (ASF) is presented as a linear combination of configuration-state functions (CSF). For example, for the final atomic ion after the Auger decay the state α having the total angular momentum JM, can be represented by the ASF

$$|\alpha;JM\rangle = \sum_{\beta=1}^{n} c^J_{\beta\alpha} |\beta;JM\rangle ,$$

TABLE I. Values for the determination of the energies of the M_4-$N_{2,3}N_{2,3}(^1S_0)$ and M_5-$N_1N_{2,3}(^1P_1)$ Auger lines of Kr.

Kr I	Ionization potential:[11,12]	112 914.5 cm^{-1}
Kr II	Ionization potential:[12]	196 475.4 cm^{-1}
	Energy level $3d^94s^24p^6,{}^2D_{5/2}$:[13]	93.788 eV
	Energy level $3d^94s^24p^6,{}^2D_{3/2}$:[13]	95.038 eV
Kr III	Energy level $4s^24p^4,{}^1S_0$:[11,14]	33 079 cm^{-1}
	Energy level $4s^14p^5,{}^1P_1$:[11,14]	141 876 cm^{-1}

TABLE II. Experimental and calculated energies of the $3d$ Auger transitions of Kr.

Single config. designation	Experimental Werme M_5	Werme M_4	Mehlhorn M_5	Mehlhorn M_4	This work Abs. energy Line in Fig. 1	M_5	Line in Fig. 1	M_4	This work Rel. energy (This work)	Optic	Calc. Abs. energy M_5	M_4	Calc. Rel. energy	Wave function of the final state (Table III)
$M_{4,5}$-$N_1N_1(^1S_0)$					1	14.71	2	15.94	−38.91		13.89	15.13	−39.96	ψ_1
	24.18	25.45	24.21	25.45	7	24.20	8	25.45	−29.41		26.01	27.24	−27.84	ψ_2
	29.59	30.84	29.61	30.89	17	29.60	19	30.85	−24.01		27.93	29.16	−25.92	ψ_3
	31.09	32.34	31.11	32.35	20	31.11	23	32.35	−22.51	−22.55	29.99	31.22	−23.86	ψ_4
	32.98	34.23	32.99	34.24	25	33.00	28	34.21	−20.62	−20.78	31.14	32.37	−22.71	ψ_5
$M_{4,5}$-$N_1N_{2,3}(^1P_1)$	37.87	38.91	37.87	39.11	29	37.84	30	39.08	−15.78	−15.78	38.28	39.51	−15.57	ψ_6
$M_{4,5}$-$N_1N_{2,3}(^3P_0)$	40.39	41.89	40.40	41.88	31	40.36	34	41.85	−13.25	−13.25	41.56	42.79	−12.29	ψ_7
$M_{4,5}$-$N_1N_{2,3}(^3P_1)$	40.66	42.34	40.66	42.32	32	40.63	35	42.31	−12.98	−12.99	41.42	42.65	−12.43	ψ_8
$M_{4,5}$-$N_1N_{2,3}(^3P_2)$	41.09		41.10		33	41.07			−12.54	−12.56	41.95	43.19	−11.90	ψ_9
$M_{4,5}$-$N_{2,3}N_{2,3}(^1S_0)$	51.35	52.61	51.36	52.59	46	51.33	48	52.58	−2.28	−2.29	51.11	52.33	−2.74	ψ_{10}
$M_{4,5}$-$N_{2,3}N_{2,3}(^1D_2)$	53.65	54.90	53.64	54.86	49	53.61	50	54.85	0.00	0.00	53.85	55.08	0.00	ψ_{11}
$M_{4,5}$-$N_{2,3}N_{2,3}(^3P_0)$	54.90	56.14	54.86	56.01	50	54.85	52	56.11	1.23	1.16	55.32	56.56	1.47	ψ_{12}
$M_{4,5}$-$N_{2,3}N_{2,3}(^3P_1)$	54.90	56.14	54.86	56.12	50	54.85	52	56.11	1.23	1.25	55.45	56.68	1.60	ψ_{13}
$M_{4,5}$-$N_{2,3}N_{2,3}(^3P_2)$	55.46	56.71	55.43	56.68	51	55.43	53	56.69	1.82	1.82	56.00	57.23	2.15	ψ_{14}

FINAL-STATE ENERGY LEVELS

FIG. 2. Energy-level structure of the doubly ionized krypton obtained from single-manifold and multiconfiguration Dirac-Fock calculations, Auger-electron spectroscopy, and optical spectroscopy. The designations in the multiconfiguration DF results refer to the configuration which makes a dominant contribution to the eigenvector.

where n is the number of CSF's included in the expansion and $c_{\beta\alpha}^J$ are the configuration mixing coefficients for state α. The CSF's $|\beta;JM\rangle$ are built from central field spinors and correspond to a pure jj-coupled state. The self-consistent-field approach results in multiconfiguration Dirac-Fock (MCDF) equations which are solved using the package of Grant et al.[17]

Single-manifold Dirac-Fock calculations were first carried out for all the final states participating in the Auger transitions. A manifold of CSF consist of all CSF map-

ping into the same nonrelativistic configuration. The final-state manifolds for the doubly ionized ion core are $4s^04p^6$, $J=0$; $4s^14p^5$, $J=0,1,2$, and $4s^24p^4$, $J=0,1,2$.

As the next step, multiconfiguration calculations including the interaction with certain excited states were performed for the final s-hole states. The manifolds used in calculations carried out for positive parity, were $4s^04p^6$, $4s^14p^44d^1$, $4s^24p^24d^2$, $4s^14p^45s^1$, $4s^24p^24d^15s^1$, $4s^24p^25s^2$, and for negative parity, $4s^14p^5$, $4s^24p^34d^1$, $4s^24p^35s^1$.

TABLE III. Wave functions of the final state of the $3d$ Auger transitions of Kr.

$\psi_1 = 0.618 \mid 4s^04\bar{p}^24p^44\bar{d}^04d^05s^0, J=0 \rangle + 0.281 \mid 4s^14\bar{p}^14p^34\bar{d}^14d^05s^0, J=0 \rangle + 0.221 \mid 4s^14\bar{p}^14p^34\bar{d}^14d^05s^0, J=0 \rangle$
$\qquad - 0.426 \mid 4s^14\bar{p}^14p^34\bar{d}^04d^15s^0, J=0 \rangle - 0.279 \mid 4s^14\bar{p}^24p^24\bar{d}^14d^05s^0, J=0 \rangle + 0.347 \mid 4s^14\bar{p}^24p^24\bar{d}^04d^15s^0, J=0 \rangle$

$\psi_2 = -0.427 \mid 4s^04\bar{p}^24p^44\bar{d}^04d^05s^0, J=0 \rangle + 0.695 \mid 4s^24\bar{p}^14p^14\bar{d}^04d^25s^0, J=0 \rangle + 0.299 \mid 4s^24\bar{p}^14p^14\bar{d}^24d^05s^0, J=0 \rangle$

$\psi_3 = -0.401 \mid 4s^14\bar{p}^14p^44\bar{d}^04d^05s^0, J=1 \rangle - 0.493 \mid 4s^14\bar{p}^24p^34\bar{d}^04d^05s^0, J=1 \rangle - 0.496 \mid 4s^24\bar{p}^04p^34\bar{d}^04d^05s^0, J=1 \rangle$
$\qquad - 0.408 \mid 4s^24\bar{p}^14p^24\bar{d}^14d^05s^0, J=1 \rangle - 0.325 \mid 4s^24\bar{p}^24p^14\bar{d}^04d^15s^0, J=1 \rangle$

$\psi_4 = 0.311 \mid 4s^14\bar{p}^14p^44\bar{d}^04d^05s^0, J=1 \rangle + 0.393 \mid 4s^14\bar{p}^24p^34\bar{d}^04d^05s^0, J=1 \rangle - 0.357 \mid 4s^24\bar{p}^04p^34\bar{d}^04d^15s^0, J=1 \rangle$
$\qquad - 0.431 \mid 4s^24\bar{p}^04p^34\bar{d}^14d^05s^0, J=1 \rangle - 0.286 \mid 4s^24\bar{p}^14p^24\bar{d}^14d^05s^0, J=1 \rangle - 0.245 \mid 4s^24\bar{p}^14p^24\bar{d}^14d^05s^0, J=1 \rangle$
$\qquad - 0.411 \mid 4s^24\bar{p}^14p^24\bar{d}^04d^15s^0, J=1 \rangle - 0.310 \mid 4s^24\bar{p}^24p^14\bar{d}^04d^15s^0, J=1 \rangle$

$\psi_5 = 0.385 \mid 4s^14\bar{p}^14p^44\bar{d}^04d^05s^0, J=1 \rangle - 0.346 \mid 4s^14\bar{p}^24p^34\bar{d}^04d^05s^0, J=1 \rangle + 0.441 \mid 4s^24\bar{p}^04p^34\bar{d}^04d^15s^0, J=1 \rangle$
$\qquad - 0.214 \mid 4s^24\bar{p}^04p^34\bar{d}^14d^05s^0, J=1 \rangle - 0.256 \mid 4s^24\bar{p}^14p^24\bar{d}^14d^05s^0, J=1 \rangle - 0.316 \mid 4s^24\bar{p}^14p^24\bar{d}^04d^15s^0, J=1 \rangle$
$\qquad + 0.496 \mid 4s^24\bar{p}^14p^24\bar{d}^14d^05s^0, J=1 \rangle$

$\psi_6 = -0.401 \mid 4s^14\bar{p}^14p^44\bar{d}^04d^05s^0, J=1 \rangle - 0.391 \mid 4s^14\bar{p}^24p^34\bar{d}^04d^05s^0, J=1 \rangle + 0.241 \mid 4s^24\bar{p}^04p^34\bar{d}^04d^15s^0, J=1 \rangle$
$\qquad - 0.203 \mid 4s^24\bar{p}^04p^34\bar{d}^14d^05s^0, J=1 \rangle - 0.374 \mid 4s^24\bar{p}^14p^24\bar{d}^14d^05s^0, J=1 \rangle - 0.528 \mid 4s^24\bar{p}^14p^24\bar{d}^04d^15s^0, J=1 \rangle$
$\qquad + 0.343 \mid 4s^24\bar{p}^24p^14\bar{d}^14d^05s^0, J=1 \rangle$

$\psi_7 = -0.841 \mid 4s^14\bar{p}^14p^44\bar{d}^04d^05s^0, J=0 \rangle - 0.336 \mid 4s^24\bar{p}^04p^34\bar{d}^14d^05s^0, J=0 \rangle - 0.292 \mid 4s^24\bar{p}^14p^24\bar{d}^14d^05s^0, J=0 \rangle$
$\qquad + 0.306 \mid 4s^24\bar{p}^14p^24\bar{d}^04d^15s^0, J=0 \rangle$

$\psi_8 = 0.642 \mid 4s^14\bar{p}^14p^44\bar{d}^04d^05s^0, J=1 \rangle - 0.547 \mid 4s^14\bar{p}^24p^34\bar{d}^04d^05s^0, J=1 \rangle - 0.223 \mid 4s^24\bar{p}^04p^34\bar{d}^04d^15s^0, J=1 \rangle$
$\qquad - 0.208 \mid 4s^24\bar{p}^14p^24\bar{d}^04d^15s^0, J=1 \rangle - 0.348 \mid 4s^24\bar{p}^14p^24\bar{d}^14d^05s^0, J=1 \rangle + 0.210 \mid 4s^24\bar{p}^24p^14\bar{d}^14d^05s^0, J=1 \rangle$

$\psi_9 = 0.847 \mid 4s^14\bar{p}^24p^34\bar{d}^04d^05s^0, J=2 \rangle - 0.298 \mid 4s^24\bar{p}^14p^24\bar{d}^04d^15s^0, J=2 \rangle + 0.227 \mid 4s^24\bar{p}^14p^24\bar{d}^14d^05s^0, J=2 \rangle$
$\qquad + 0.264 \mid 4s^24\bar{p}^24p^14\bar{d}^04d^15s^0, J=2 \rangle$

$\psi_{10} = -0.709 \mid 4s^24\bar{p}^14p^3, J=0 \rangle - 0.706 \mid 4s^24\bar{p}^24p^2, J=0 \rangle$

$\psi_{11} = -0.901 \mid 4s^24\bar{p}^14p^3, J=2 \rangle + 0.434 \mid 4s^24\bar{p}^24p^2, J=2 \rangle$

$\psi_{12} = 0.706 \mid 4s^24\bar{p}^04p^4, J=0 \rangle - 0.709 \mid 4s^24\bar{p}^24p^2, J=0 \rangle$

$\psi_{13} = -1.000 \mid 4s^24\bar{p}^14p^3, J=1 \rangle$

$\psi_{14} = 0.434 \mid 4s^24\bar{p}^14p^3, J=2 \rangle + 0.901 \mid 4s^24\bar{p}^24p^2, J=2 \rangle$

The final-state energy levels obtained from single-manifold and multiconfiguration calculations are compared with experiment in Fig. 2. The final-state wave functions (ASF) are listed in Table III.

IV. DISCUSSION

The experimental energies of the $M_{4,5}$-$N_{2,3}N_{2,3}$ transitions were found to be lower by about 0.2 eV than the values obtained with the single-manifold Dirac-Fock approach. This difference arises from the deviations between experiment and theory both in the initial and in the final states. The energies of the ...$3d^9 4s^2 4p^6(^2D_{5/2})$ initial state were found to be 93.79 and 92.18 eV and the energies of the ...$3d^{10} 4s^2 4p^4(^1D_2)$ final state 40.18 and 38.33 experimentally and theoretically, respectively. The deviations in the initial- and final-state binding energies are of the same magnitude and thus cancel when the Auger energies are obtained as the energy difference. The calculated initial-state spin-orbit splitting of 1.23 eV agrees well with the experimental value of 1.25 eV. Furthermore, the calculated final-state energy splitting appears to be larger by about 0.8 eV than the experimental value. However, the single-manifold estimation seems to reproduce the observed energy structure of the $M_{4,5}$-$N_{2,3}N_{2,3}$ transitions reasonably well.

The multiconfiguration calculations carried out for the $M_{4,5}$-N_1N_1 and $M_{4,5}$-$N_1N_{2,3}$ transitions show that there is strong interaction between $4s^0 4p^6$, $4s^1 4p^4 4d^1$, and $4s^2 4p^2 4d^2$ manifolds of positive parity and between $4s^1 4p^5$ and $4s^2 4p^3 4d^1$ manifolds of negative parity. This effect causes large energy shifts as can be seen from Fig. 2, and considerable mixing of CSF's as can be seen from the configuration-mixing coefficients in Table III. The $4s^1 4p^4 5s^1$, $4s^2 4p^2 5s^2$, and $4s^2 4p^3 5s^1$ manifolds, on the other hand, are almost unperturbed. For some ASF the extent of configuration mixing is so great that the single-manifold assignment presented in Fig. 2 is of purely notational value, since no single-manifold term dominates in ASF. We therefore prefer to describe states with their ASF's given in Table III.

Comparison between experimental and calculated energies of the $M_{4,5}$-$N_1N_{2,3}$ transitions (Table II) shows that the calculated Auger energies of the $M_{4,5}$-$N_1N_{2,3}(^1P_1,^3P_{0,1,2})$ lines are 0.4—0.9 eV higher than the experimental energies. On the other hand, the energies of the satellite lines, which are caused by the final-state interaction with the $^1P_1$ line, are slightly underestimated by theory. The initial- and final-state binding energies cause these differences: initial-state energies are slightly underestimated in theory, final-state energies of the satellite levels agree well (Fig. 2), whereas the energies of the normal states are considerably underestimated. The same trend is observed in the case of the $M_{4,5}$-N_1N_1 transitions.

The mixing of the $4s^0 4p^6$, $4s^1 4p^4 4d^1$, and $4s^2 4p^2 4d^2$ manifolds and of the $4s^1 4p^5$ and $4s^2 4p^3 4d^1$ manifolds predicted by the multiconfiguration Dirac-Fock calculations seems to reproduce the observed structure but results in slightly too strong energy shifts. The redistribution of the intensity, if approximated by the squares of the mixing coefficients, is also somewhat overestimated. It is clear that, in order to arrive at a complete description of the energy-level structure, it is necessary to include the interaction with the continuum, as well as the other weaker interactions, both in the initial and in the final states.

Our multiconfiguration calculations support the same reinterpretation of the $M_{4,5}$-$N_1N_{2,3}$, $J=1$ and $M_{4,5}$-N_1N_1, $^1S_0$ lines that was pointed out in Refs. 1 and 4. Furthermore, the intensity of the $M_{4,5}$-N_1N_1, $^1S_0$ transitions is also found to be redistributed between the transitions to the final states with $J=0$. Calculations indicate further structure at lower energy which, however, has not been observed experimentally due to the strong background in the 0—10 eV energy region.

Apart from the main lines labeled in Table II, several low-intensity lines are observed experimentally (Fig. 1) but not identified in detail; multiconfiguration calculations indicate several additional satellites arising from configuration interaction with the $4s^0 4p^6$ and $4s^1 4p^5$ manifolds, but with very small intensities. The autoionization lines with a $5p$ spectator electron may lie on the high-energy side of the main lines. The satellite Auger transitions, where the double-hole states decay to the triple-hole states, accompany the normal Auger transitions on their low-energy side.

[1]E. J. McGuire, Phys. Rev. A 11, 17 (1975); 11, 1880 (1975).

[2]K. G. Dyall, and F. P. Larkins, J. Phys. B 15, 203 (1982); 15, 219 (1982).

[3]J. E. Hansen, Comments At. Mol. Phys. 12, 197 (1982).

[4]K. G. Dyall, and F. P. Larkins, J. Phys. B 15, 2793 (1982); in Inner-shell and x-Ray Physics of Atoms and Solids, edited by D. J. Fabian, H. Kleinpoppen, and M. Watson, (Plenum, New York, 1981), p. 265.

[5]L. O. Werme, T. Bergmark, and K. Siegbahn, Phys. Scr. 6, 141 (1972).

[6]S. Southworth, U. Becker, C. M. Truesdale, P. H. Kobrin, D. W. Lindle, S. Owaki, and D. A. Shirley, Phys. Rev. A 28, 261 (1983).

[7]H. Aksela, S. Aksela, and H. Pulkkinen, Phys. Rev. A 30, 865 (1984).

[8]W. Mehlhorn, W. Schmitz, and D. Stalherm, Z. Phys. 252, 399 (1972).

[9]H. Derenbach, and V. Schmidt, J. Phys. B 17, 83 (1984).

[10]J. Väyrynen, and S. Aksela, J. Electron Spectrosc. 16, 423 (1979).

[11]C. E. Moore, Atomic Energy Levels, Natl. Bur. Stand. (U.S.) Circ. No. 467 (U.S. GPO, Washington D.C., 1949, 1952, and

1958), Vols. I—III.

[12]B. Petersson, Ark. Fys. Semin. Trondheim **27**, 317 (1964).

[13]G. C. King, M. Tronc, F. H. Read, and R. C. Bradford, J. Phys. B **10**, 2479 (1977).

[14]L. Minnhagen, H. Strihed, and B. Pettersson, Ark. Fys. Semin. Trondheim **39**, 471 (1969).

[15]J. E. Hansen, and W. Persson, Phys. Rev. A **20**, 364 (1979).

[16]S. Ohtani, H. Nishimura, H. Suzuki, and K. Wakiya, Phys. Rev. Lett. **36**, 863 (1976).

[17]I. P. Grant, B. J. Kenzie, and P. H. Norrington, Comput. Phys. Commun. 21, 207 (1980); 21, 233 (1980).